CHEMISTRY
AN ASIAN JOURNAL

www.chemasianj.org

Accepted Article

Title: DFT mechanistic insights into the Ni(II)-catalyzed enantioselective arylative cyclization of tethered allene-ketones

Authors: Chi Bong Eric Chao, Stephen G. Pyne, Christopher J. T. Hyland, and Richmond Lee

To be cited as: *Chem. Asian J.* **2023**, e202300724

Link to VoR: https://doi.org/10.1002/asia.202300724

A Journal of

ACES
Asian Chemical Editorial Society

WILEY VCH

10.1002/asia.202300724

WILEY VCH

RESEARCH ARTICLE

DFT mechanistic insights into the Ni(II)-catalyzed enantioselective arylative cyclization of tethered allene-ketones

Chi Bong Eric Chao,[a,b] Stephen G. Pyne,*[a,b] Christopher J. T. Hyland*[a,b] and Richmond Lee*[a,b]

[a] C. B. E. Chao, Prof. Dr. S. G. Pyne, Prof. Dr. C. J. T. Hyland, Prof. Dr. R. Lee
School of Chemistry and Molecular Bioscience
University of Wollongong, Wollongong, NSW 2522, Australia
E-mail: spyne@uow.edu.au; chrhyl@uow.edu.au; richmond_lee@uow.edu.au

[b] Molecular Horizons, University of Wollongong, Wollongong, NSW 2522, Australia

Supporting information for this article is given via a link at the end of the document

Abstract: Density functional theory (DFT) has provided a detailed mechanistic picture for the redox neutral nickel(II)-catalyzed arylative cyclization reactions of a tethered allene–ketone with arylboronic acids. A mechanistic rationale for the high diastereo- and enantioselectivity achieved experimentally at high reaction temperature was uncovered through modeling the reaction with a chiral ligand and the predicted stereochemical outcome corroborates with experimental results. An unprecedented pathway for the base-free organoboron transmetalation pathway was revealed and the regioselectivity of migratory insertion of tethered allene-ketones as well as the stability of the possible allylnickel isomers (σ-allyl vs π–allyl) were clarified. The multifaceted nature of the reaction is revealed with certain elementary steps preferring cationic compared to the neutral state.

Introduction

Allenes are versatile molecular building blocks[1, 2] and their reactivity in the presence of coinage metal-catalysts has been widely explored.[3] In contrast, reactions of allenes catalyzed by abundant, first-row transition metal catalysts, such as nickel are only just starting to emerge.[4] Many of these processes invoke a Ni(0)/Ni(II) redox cycle but far less use a redox neutral Ni(II) system and of these very few investigations involve diastereo- and enantioselective variants.[5-11] In 2020, the Lam group developed a highly enantio- and diastereoselective Ni(II)-catalyzed arylative cyclization reactions of tethered allene-ketones to form biologically important pyrrolidinones, pyrrolidines, piperidines, cyclohexanes and cyclopentanes, while avoiding the use of air-sensitive Ni(0) catalysts. Proposed key steps in this reaction included: (i) transmetalation of the arylboronic acid to Ni(II), followed by (ii) migratory insertion of the resulting aryl-nickel species with the allene substrate to form a (iii) nucleophilic σ-allylnickel species for the cyclization step (Scheme 1A – showing formation of pyrrolidinone **PDT** as a representative example).[12] Intriguingly, Lam and co-workers demonstrated that these reactions were performed in the absence of a base;[12] which is unusual given that the transmetalation between arylboronic acids and Ni(II) complexes typically requires a base to form an activated boronate complex.[13] Base-free transmetalation processes with Pd(0) and Ni(0) systems have recently been discovered for cross-coupling reactions in the presence of fluoride ion, where the strong fluorophilicity of boron facilitates the base-free transmetalation reaction.[14-16] The addition of a ketone in place of a strong base was found to also facilitate the transmetalation reaction in Ni(0)-catalyzed coupling reactions but this requires stoichiometric amounts of the ketone making this process not atom economical.[17]

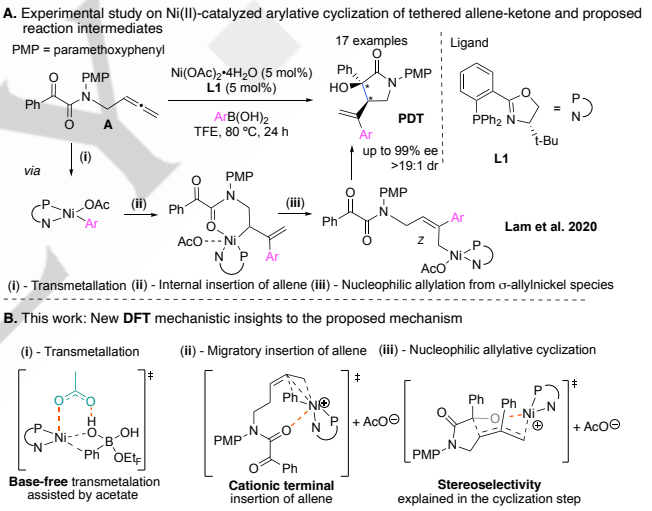

Scheme 1. (A) Experimental work on redox neutral Ni(II)-catalyzed arylative cyclization of tethered allene-ketone with key proposed intermediates by Lam. (B) This work on the mechanistic studies of the aforementioned reaction with new insights through DFT calculations.

Although there are some advances in base-free transmetalation reactions, they have been limited to Pd(0)/Pd(II) / Ni(0)/Ni(II) redox coupling reactions only. The post-transmetalation allene migratory insertion – (ii) in Scheme 1A – also raises interesting mechanistic questions, notably concerning the regioselectivity, which can occur either at the terminal or internal π-bond with Lam and co-workers proposing that the carbonyl group on the amide directed the regioselectivity to the internal position to form a nucleophilic σ-allyl complex.[18] The exact nature of this nucleophilic intermediate that undergoes the ring-forming reaction with remarkably high diastereo- and enantioselectivity of this process at high reaction temperature of 80 °C is also intriguing and warrants detailed study.

10.1002/asia.202300724

RESEARCH ARTICLE

Herein, we present the results and findings of our DFT studies on the enantioselective Ni(II)-catalyzed arylative 1,2-allylations of the tethered allene-ketone system **A**, the key elementary steps for this transformation involve (i) base-free transmetalation, (ii) cationic terminal allene insertion, and (iii) a diastereo- and enantio-determining cyclization step (Scheme 1B).

Results and Discussion

Proposed mechanism by Lam and co-workers

To account for the experimental observations of the arylative cyclization reaction of allene **A**, Lam and co-workers proposed that once the active chiral nickel complex **int-I** is formed (Scheme 2), transmetalation with phenylboronic acid results in the phenylnickel species **int-II**. This is followed by an internal migratory insertion of the allene starting material to form σ-allylnickel species **int-III** which interconverts by σ–π–σ isomerization to a preferable (*Z*)-σ-allylnickel **int-IV-a** over (*E*)-σ-allylnickel **int-IV-b** based on the stereochemical outcome of the reaction. Intramolecular nucleophilic allylation then occurs through a chelated 5,6–bicyclic ring intermediate in the cationic (*Z*)-σ-allylnickel species **int-V** through dissociation and reassociation of the anionic acetate ligand to give nickel alkoxide **int-VI** that can then undergo protonolysis to release the observed pyrrolidine-2-one product (**PDT**) and regenerate active catalyst **int-I**.

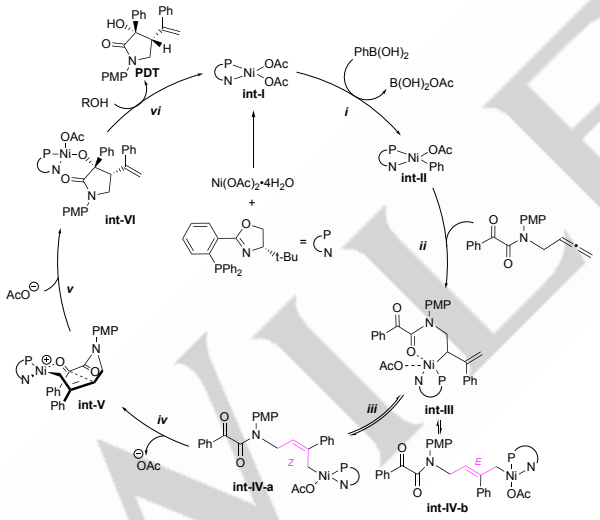

Scheme 2. Reaction mechanism proposed by Lam and co-workers for Ni(II)-catalyzed arylative cyclization reaction shown in Scheme 1A.

Modelling possible base-free organoboron transmetalation pathways

Previous computational studies have indicated that the base-mediated transmetalation reaction in nickel systems occurs through a four-membered ring boronate transition state (TS) structure.[19, 20] A more recent detailed experimental and DFT mechanistic study by Perego, Ciofini and Grimaud also proposed this key four-membered transition state for the transmetalation process with hydroxide as mediator.[21] As the use of stoichiometric amounts of strong base in these reactions could induce undesired side reactions and limit the substrate scope,[22] the importance on elucidating the mechanism of the base-free transmetalation under Lam's experimental conditions is critical in the future advances in organoboron transmetalation reactions.

Our initial calculations involved the use of achiral ligand, 2-(2-(diphenylphosphaneyl)phenyl)-4,5-dihydrooxazole, **L2**, which is from phosphinooxazoline ligand class (Scheme 3) to computationally investigate the feasibility of the reaction mechanism in step *i* of Scheme 2. Our initial calculations investigated the possibility of generating the Ni(II)-boronate intermediate **1a** from $Ni(OAc)_2$ (**1**) and two equivalents of phenylboronic acid (**B1**) under base-free conditions (Scheme 3A), since a negatively charged boronate would be activated to allow the aryl group transfer to the Ni metal more easily. However, the solution free energy, in trifluoroethanol (TFE) as solvent calculated to generate **1a** is highly endergonic, ΔG_{sol} = 41.8 kcal/mol, with a corresponding free energy barrier for transmetalation, **TS-1a**, of $\Delta G_{sol}^{\ddagger}$ = 46.4 kcal/mol. Alternatively, the weakly basic acetate group on the nickel could potentially be involved with activating the boron for transmetalation (Scheme 3B).

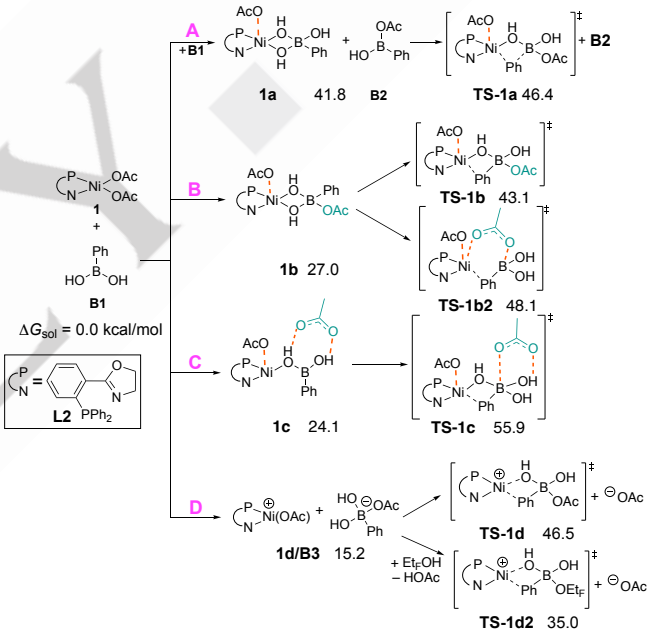

Scheme 3. Calculated pathways for the investigation on pre-transmetalation intermediates and transition states of base-free transmetalation. (A) Generation of additional hydroxy group, (B) exploration of the role of acetate group, (C) further exploration of the role of acetate group, (D) charged complexes M06/def2TZVP+QZVP/SMD(2,2,2-TriFluoroEthanol)//M06/6-31G(d,p)+SDD level of theory. Values are solution free energies in kcal/mol with reference to complex **1** and starting material arylboronic acid **B1**. PN ligand = L2 = achiral PHOX = 2-(2-(diphenylphosphaneyl)phenyl)-4,5-dihydrooxazole. Coordinate bonds are represented as orange-colored dashed lines.

In this regard, the calculated free energy for intermediate **1b** where the acetate replaces the hydroxy group on the boronate ligand, ΔG_{sol} = 27.0 kcal/mol, is endergonic but is lower in free energy than **1a**. The transmetalation barrier through **TS-1b** however is still high at $\Delta G_{sol}^{\ddagger}$ = 43.1 kcal/mol. Alternatively, the acetate could act as a bridge between the nickel and oxophilic boron,[23] freeing the bridging hydroxy group to activate the boronate complex. However, the free energy required to

10.1002/asia.202300724

RESEARCH ARTICLE

overcome this barrier, **TS-1b2**, is even higher at $\Delta G_{sol}^{\ddagger}$ = 48.1 kcal/mol making it unviable. This barrier is much higher in contrast to a reported base-free Pd(II)-catalyzed transmetalation aided by acetate,[24] suggesting fundamental differences in reactivity between Pd(II) and Ni(II). This also indicates that the hydroxy bridge stabilizes **TS-1b** by 5.0 kcal/mol or about four orders of magnitude relative to **TS-1b2**. Further roles of the acetate group and charged species such as cationic nickel complexes **1d** and boronates **B3** were explored as alternative pathways (Scheme 3C, and 3D). The optimized structure of intermediate **1c** (ΔG_{sol} = 24.1 kcal/mol) was observed to have hydrogen bonding interactions between the acetate and hydroxy groups on the boron to form a bridged structure but the following **TS-1c** requires a barrier of $\Delta G_{sol}^{\ddagger}$ = 55.9 kcal/mol to overcome resulting in another high energy pathway. The generation of charged separated species, **1d/B3**, requires 15.2 kcal/mol of energy and is relatively less endergonic but the cationic **TS-1d** is still high at $\Delta G_{sol}^{\ddagger}$ = 46.5 kcal/mol. Given the relatively high concentration of trifluoroethanol, an alternative TS (**TS-1d2**) was considered in assisting the transmetalation step. The energy is lower at $\Delta G_{sol}^{\ddagger}$ = 35.0 kcal/mol, but still too high to be viable. However, it is worth noting that the charged separated intermediates **1d/B3** has the most favorable free energy compared to other pre-transmetalation intermediates **1a, 1b** and **1c**.

With the computational screening of different pathways for this base-free transmetalation step establishing pathway **D** with the most favorable charge separated intermediate **1d/B3**, we wondered if the acetate group could further assist in the aryl transfer by deprotonating the bridging O–H (Figure 1).[25] Previous experimental and theoretical studies on palladium acetate precatalysts indicated that acetate was crucial in acting as a base in sub-stoichiometric amounts, highlighting that a low concentration of acetate is sufficient for such a process.[26] First, the arylboronic acid coordinates to the Ni(II) forming **intm-pre-1e**, ΔG_{sol} = 9.6 kcal/mol, and addition of the acetate to the boron through **TS-pre-1e** ($\Delta G_{sol}^{\ddagger}$ = 24.7 kcal/mol) accesses the pre-transmetalation complex **1e** (ΔG_{sol} = 18.1 kcal/mol). This is followed by a ligand exchange of acetate with TFE generating a more energetically favorable intermediate **1f**. Both **1e** and **1f** could then undergo transmetalation where the axially bound acetate group on the nickel deprotonates the bridging hydroxy group, and the corresponding free energy barriers for **TS-1e** is $\Delta G_{sol}^{\ddagger}$ = 31.0 kcal/mol and for **TS-1f** is $\Delta G_{sol}^{\ddagger}$ = 26.6 kcal/mol. The subsequent aryl transferred intermediates **pre-2e** and **pre-2f** are computed to have ΔG_{sol} values of 16.6 and 10.7 kcal/mol, respectively. However, the more energetically viable route would be through **TS-1f** leading to **pre-2f**, which undergoes deprotonation and ligand exchange to form complex **2** and the boron species by-product which has a free energy of –10.5 kcal/mol relative to **1** + **B1** (refer to the Supporting Information Scheme S1 for formation of other less favored post-transmetalation by-products). In general, free energies observed with TFE activating the boron across in each intermediate and TS for the transmetalation step are lower. This highlights the importance of using TFE as the solvent for this reaction which is evident from the solvent screen in Lam's work in which TFE gave a substantially higher product yield. In other reaction solvents employed by Lam that gave moderate yield, the free energy barrier for **TS_1e** is predicted to be lower and feasible, for example, calculations using a SMD solvent model for 1,4-dioxane and acetonitrile gave $\Delta G_{sol}^{\ddagger}$ = 25.9 kcal/mol and 28.7 kcal/mol, respectively. Other possible intermediates were also considered computationally due to the possibility of different binding configurations of the bidentate P-N ligand, **L2** in the square planar nickel complex **1f**. Diastereomers arising from the boron stereogenic center were also considered in the transmetalation step, however we found that **TS-1f** was the most favorable (see Supporting Information).

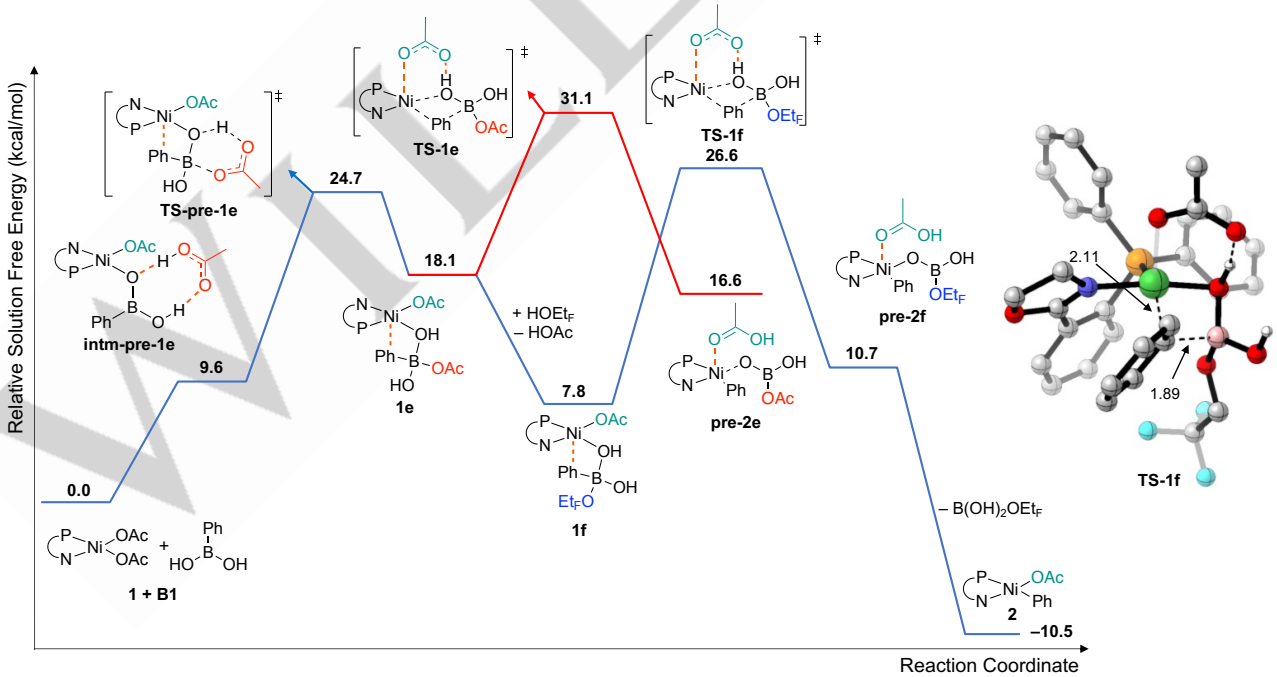

Figure 1. Energy profile calculated for the base-free transmetalation between nickel complex **1** and phenylboronic acid **B1,** with 3-dimensional ball-and-stick structure of **TS-1f** highlighting the interaction and key bond lengths. M06/def2TZVP+QZVP/SMD(2,2,2-TriFluoroEthanol)//M06/6-31G(d,p)+SDD level of theory. Values are solution free energies in kcal/mol with reference to complex **1** and starting material phenylboronic acid **B1**. PN ligand = L2 = achiral PHOX = 2-(2-(diphenylphosphaneyl)phenyl)-4,5-dihydrooxazole. 3-D structure with most Hs omitted for clarity are colour-coded, representing C (gray), N (dark blue), O (red), F (light blue), P (yellow) B (pink) and Ni (green) rendered by Cylview,[27] key bond distances in Å. Coordinate bonds are represented as orange-colored dashed lines.

10.1002/asia.202300724

WILEY VCH

RESEARCH ARTICLE

Regioselectivity of allene insertion to the phenylnickel(II) complex 2

Step *ii* of the originally proposed catalytic cycle shown in Scheme 2 is the migratory insertion of the allene starting material to the phenylnickel(II) complex **int-II**. In addition to the originally proposed internal migratory insertion of the allene, an alternative terminal insertion process was also calculated but energy barriers for both pathways were too high for neutral catalytic intermediates and TSs (see Supporting Information). Instead, cationic migratory insertions of the allene *via* dissociation of the acetate ligand were more favorable (Scheme 4). The pre-insertion complexes **intm-2a/2b_cat,** adopts a square planar 16-electron Ni(II) structure coordinated with the allene moiety, phenyl and **L2**. The free energy barrier for the cationic internal insertion through **TS-2a_cat** was found to be $\Delta G_{sol}^{\ddagger}$ = 30.8 kcal/mol (relative to **cpx1** and **A**) and which then forms cationic σ-allylnickel intermediate **3_cat**. Alternatively, a cationic terminal insertion of the allene could occur through **TS-2b_cat** which has a lower free energy barrier of $\Delta G_{sol}^{\ddagger}$ = 28.2 kcal/mol and results in the formation of cationic σ-allylnickel intermediate **4b_cat**. The amide carbonyl group (C=O) was observed to be assisting the TS *via* weak interactions with the nickel center perpendicular to the plane of the complex in both pathways. However, due to the 2.6 kcal/mol difference in the energy barrier between these pathways, the calculations predict that the migratory insertion in step *ii* occurs *via* a cationic terminal carbon insertion pathway (pathway b).

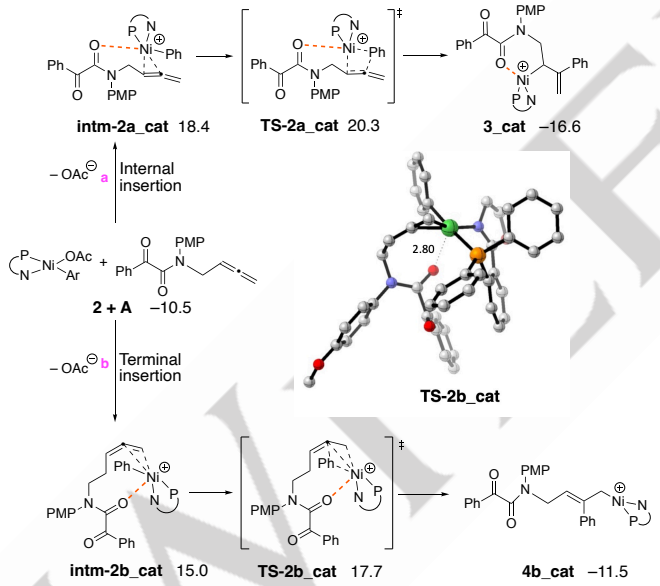

Scheme 4. Calculated pathways for the possible migratory insertion steps to form cationic allyl-nickel complexes. (a) Internal insertion of the allene to the nickel center. (b) terminal insertion of the allene to the nickel center. M06/def2TZVP+QZVP/SMD(2,2,2-TriFluoroEthanol)//M06/6-31G(d,p)+SDD level of theory. Values are solution free energies in kcal/mol with reference to complex 1 and starting material phenylboronic acid B1. PN ligand = L2 (Scheme 3) = achiral PHOX = 2-(2-(diphenylphosphaneyl)phenyl)-4,5-dihydrooxazole. 3-D structures with all H omitted for clarity are colour-coded, representing C (gray), N (dark blue), O (red), P (yellow) and Ni (green) rendered by Cylview,[27] key bond distances in Å. Coordinate bonds are represented as orange-colored dashed lines.

Diastereoselective nucleophilic allylation of ketone from the allyl-nickel complex

Upon reassociation of the acetate ligand and σ–π-σ isomerization of **4b_cat**, neutral π-allyl-Ni(II) **4b** is formed, and could undergo further σ–π-σ isomerization to form two possible isomers, *E*-**5a** and *Z*-**5b** prior to the C–C bond forming (cyclization) step. Each isomer could undergo a nucleophilic γ-allylation reaction to afford nickel alkoxide **6a** and **6b**, respectively *via* the 5,6–bicyclic ring transition states **TS-3a** and **TS-3b**, with $\Delta G_{sol}^{\ddagger}$ = 23.0 and 16.3 kcal/mol relative to **4b**, respectively. The *Z*-pathway is computed to be both kinetically ($\Delta\Delta G_{sol}^{\ddagger}$ = 6.7 kcal/mol) and thermodynamically ($\Delta\Delta G_{sol}$ = 3.2 kcal/mol) more favorable than the *E*-pathway. The reason for the difference in energies could stem from unfavorable 1,3-diaxial-like interactions in **TS-3a** between the phenyl groups and H^1. Whereas, in **TS-3b** only H^1 and the CH_2 group at C^1 are in a 1,3-diaxial disposition (see Scheme 5). The insights drawn from the computational results are congruent with the experimental results, explaining the high diastereoselectivity achieved even under the relatively high reaction temperature as the energy barrier for the *E* pathway is significantly higher. Due to the lability of the acetate ligand, cationic variations of this step were also considered, and they resulted in higher energy barriers (refer to Supporting Information).

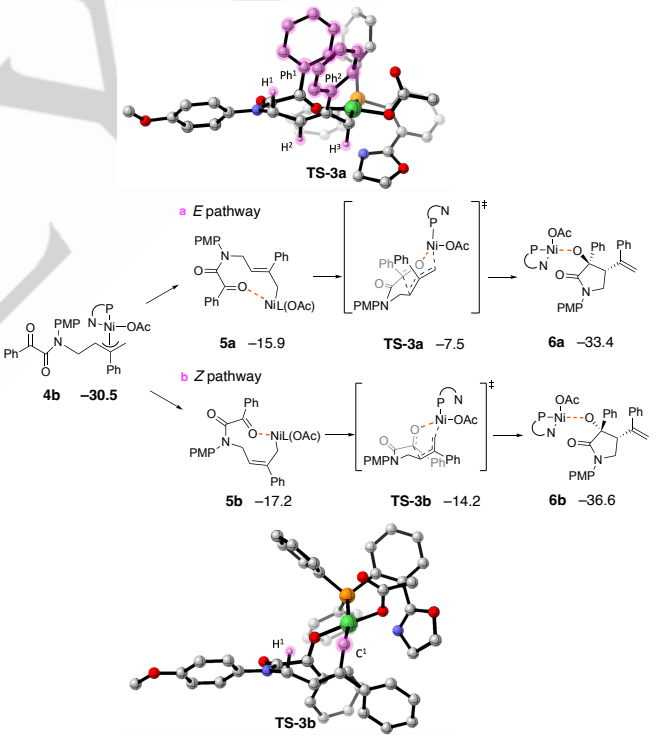

Scheme 5. Calculated pathways for the diastereoselective nucleophilic allylation to form nickel alkoxides. (a) *E*-pathway and (b) *Z*-pathway of the nucleophilic attack. M06/def2TZVP+QZVP/SMD(2,2,2-TriFluoroEthanol)//M06/6-31G(d,p)+SDD level of theory. Values are solution free energies in kcal/mol with reference to complex 1 and starting material phenylboronic acid B1. PN ligand = L2 (Scheme 3) = achiral PHOX = 2-(2-(diphenylphosphaneyl)phenyl)-4,5-dihydrooxazole. 3-D structures with most H omitted but key H and C highlighted in pink for clarity are colour-coded, representing C (gray), N (dark blue), O (red), P (yellow) and Ni (green) rendered by Cylview.[27] Coordinate bonds are represented as orange-colored dashed lines.

10.1002/asia.202300724

RESEARCH ARTICLE

Summary of the newly proposed reaction mechanism

The new proposed DFT mechanism for the nickel(II)-catalyzed arylative cyclization of tethered allene-ketone using achiral PHOX ligand **L2** is summarized in Figure 2 (neutral elementary steps in blue and cationic in red): 1) Catalyst **1** initially reacts with phenylboronic acid **B1** to generate a pre-transmetalation intermediate **1f** ; 2) followed by the base-free transmetalation reaction *via* transition state, **TS-1f** and assisted by acetate to enable aryl transfer and generate the phenylnickel **2**; 3) a carbonyl amide assisted cationic terminal insertion of the tethered allene-ketone *via* **TS-2b_cat** into **2** was found to be the rate determining step with free energy barrier of 28.2 kcal/mol. The higher energy **TS-2b** could stem from the acetate group crowding the nickel center preventing any carbonyl amide assistance. Upon acetate reassociation and σ–π-σ isomerization a stable π-allylnickel **4b** is formed; 4) Further σ–π-σ isomerization leads to a preferable *Z*-allyl-nickel intermediate **5b** that undergoes the final diastereoselective nucleophilic attack to form the nickel alkoxide **6b**. In this case, a neutral **TS-3b** is preferred over the cationic variant **TS-3b_cat** by a difference of 4.8 kcal/mol. Protodenickelation then delivers the desired pyrrolidine-2-one product and regenerates the catalyst **1**. Less energetically favorable transition states, **TS-2b** and **TS-3b_cat** for the corresponding migratory insertion and nucleophilic allylation steps are also shown (for more details, please see Supporting Information).

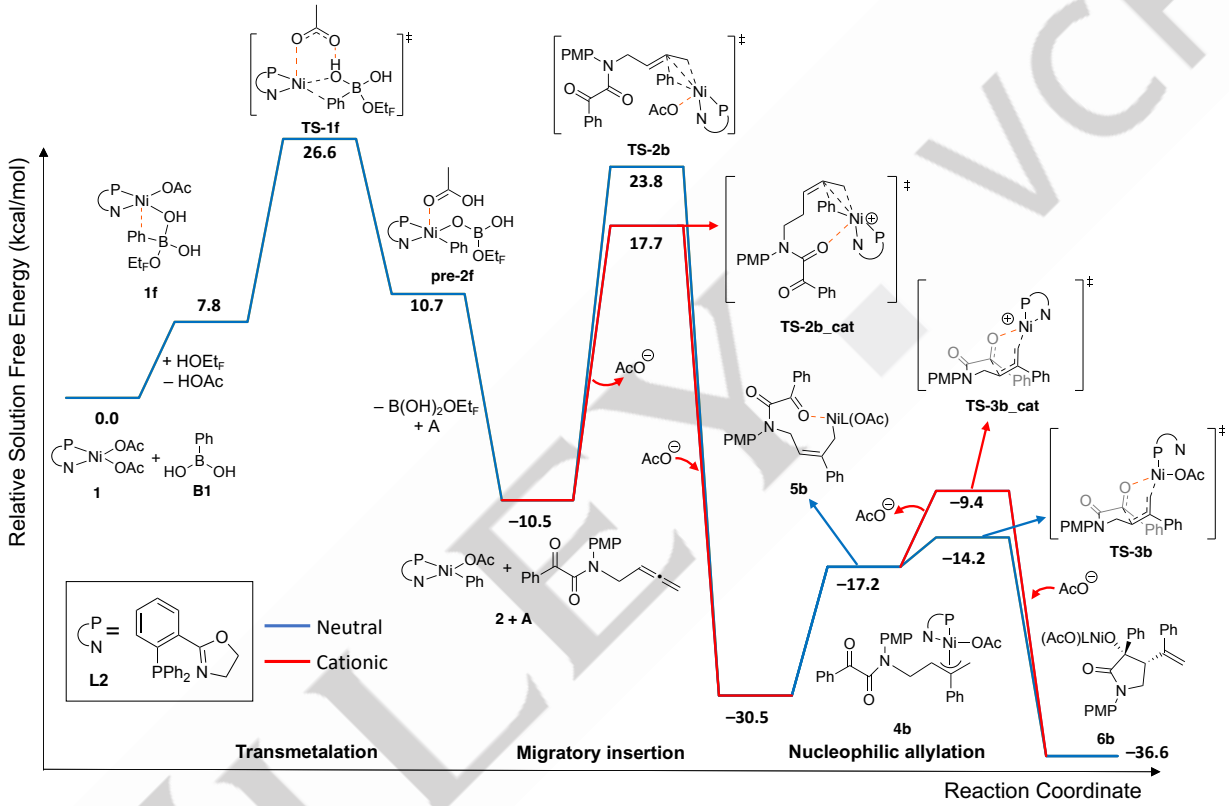

Figure 2. Energy profile of the newly proposed mechanism for Ni(II) catalyzed arylative cyclization reaction of tethered allene ketone. M06/def2TZVP+QZVP/SMD(2,2,2-TriFluoroEthanol)//M06/6-31G(d,p)+SDD level of theory. Values are solution free energies in kcal/mol with reference to complex **1** and starting material phenylboronic acid **B1**. L/ PN ligand = L2 (Scheme 3) = achiral PHOX = 2-(2-(diphenylphosphaneyl)phenyl)-4,5-dihydrooxazole. Coordinate bonds are represented as orange-colored dashed lines.

Enantioselective nucleophilic allylation of ketone from allyl-nickel complex 4b

Attention was next turned to explaining the high enantioselectivity achieved in the original experimental work using chiral PHOX ligand **L1** at 80 ºC (Scheme 6). Interestingly, the mechanism for the enantiodetermining nucleophilic attack of the Ni-allyl intermediate on the ketone moiety was found to be different for reactions employing chiral **L1** and achiral **L2,** owing to the sterically demanding *tert*-butyl substituent on the oxazoline unit of the chiral ligand. The bulkier ligand **L1** necessitates dissociation and reassociation of the acetate group in steps *iv* and *v* of Scheme 2 (refer to the Supporting Information Scheme S2 for cationic pre- and post-nucleophilic allylation cyclization intermediates and detailed stereochemical discussion), but as seen for the **L2** achiral model this was not required (Scheme 6). The effect of **L1** is most apparent for the stereoisomer **e2** and the structure of **TS3_e2** showed that the bulky *tert*-butyl group being close to the amide group and blocking the coordination site of the nickel resulting in a sterically demanding bicyclic 5,5-membered ring TS geometry, and as a result requiring a higher free energy barrier of $\Delta G_{sol}^{\ddagger}$ = 36.1 kcal/mol when compared to the other transition states adopting less strained 5,6-membered ring geometries. With the remaining three possible stereoisomers (**6_e1**, **e3** and **e4**), the calculations showed that the pathway that leads to the enantiomer with the absolute configurations of (*1S*, 2*R*) in the corresponding pyrrolidine-2-one structure was through the kinetically most favorable transition state **TS3_e4**, $\Delta G_{sol}^{\ddagger}$ =

10.1002/asia.202300724

17.3 kcal/mol, to also form the thermodynamically most stable nickel alkoxide **6_e4**, $\Delta G_{sol}^{\ddagger}$ = –14.7 kcal/mol, relative to **4b***. Although the difference in activation energies between **TS3_e3** and **TS3_e4** is only 1.1 kcal/mol, the retro-allylation reactions of **6_e3** and **6_e4** have activation energies of 25.8 and 32.0 kcal/mol, respectively. This suggests the reversible formation of **6_e3** and the irreversible formation of **6_e4**. Hence the enantioselective formation of **6_e4** is driven by both kinetic and thermodynamic factors. The absolute configuration predicted for the pyrrolidin-2-one **PDT** (Scheme 2) through theoretical calculations corroborate with the experimental X-ray crystal structure of the final product from Lam and co-workers.

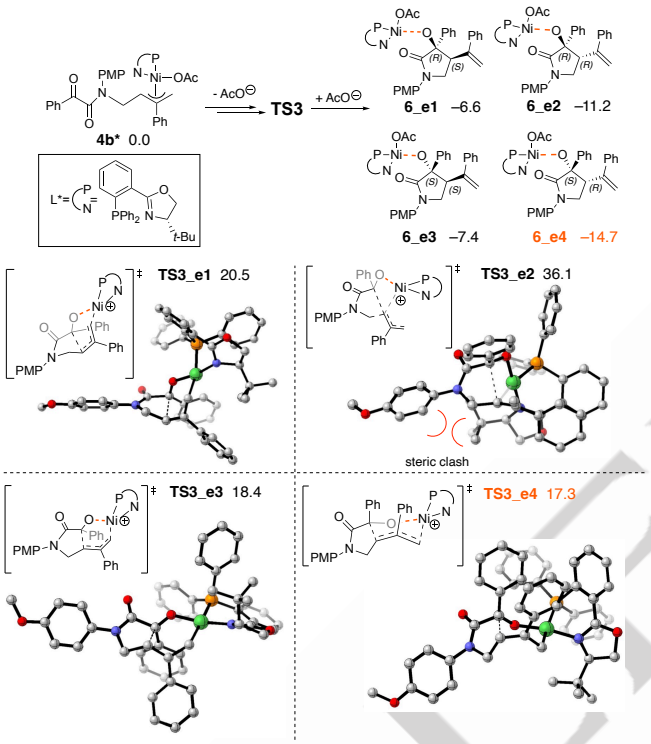

Scheme 6. Calculated pathways for the enantioselective nucleophilic allylation. M06/def2TZVP+QZVP/SMD(2,2,2-TriFluoroEthanol)//M06/6-31G(d,p)+SDD level of theory. Values are solution free energies in kcal/mol with reference to allylnickel complex **4b***. L*/ PN ligand = **L1** (Scheme 2) = chiral (*S*)-4-(*tert*-butyl)-2-(2-(diphenylphosphaneyl)phenyl)-4,5-dihydrooxazole. 3-D structures with all H omitted for clarity are colour-coded, representing C (gray), N (dark blue), O (red), P (yellow) and Ni (green) rendered by Cylview.[26] Coordinate bonds are represented as orange-colored dashed lines.

Conclusion

Through DFT modelling, a mechanism for the nickel-catalyzed arylative cyclization reaction of the tethered allene-ketone **A** is proposed with key new insights into each of the elementary steps of the reaction. Firstly, it can be concluded that the base-free organoboron transmetalation step requires involvement of the acetate groups from the nickel source and the use of trifluoroethanol as the solvent to drive the aryl transfer. The regioselectivity of the allene insertion was deduced to prefer terminal insertion with a directing effect from the amide carbonyl group through a cationic Ni(II) system, which is in contrast to the initial prediction of a neutral Ni(II) catalyst system. We have meticulously considered both possibilities of neutral and cationic pathways for all elementary steps since the acetate is labile, highlighting the multifaceted nature of the reaction. This insight along with identifying the π-allyl-Ni(II) **4b** as a key intermediate, provides critical information to allow design of Ni(II)-catalyzed reactions of allenic systems, which are valuable building blocks in organic synthesis. Lastly, analysis of the diastero- and enantioselective nucleophilic allylation showed that out of the four possible stereoisomers, the most kinetically and thermodynamically favorable TS and pyrrolidin-2-one product matches with the absolute configuration reported by Lam.

These findings will enrich the fundamental understanding of related Ni(II)-catalyzed reactions involving transmetalation with organoboron reagents and provide useful insights to the catalysis community in the future design of experiments in the studies of other such catalytic systems in the presence of unsaturated substrates.

Computational details

Grimme's CREST default iMTD-GC algorithm was used to provide conformational search of the most energetically stable structures in key intermediates, **1**, **1f** and **2.**[28] All calculations were carried out with the Gaussian 16 software package.[29] The molecular gas-phase geometry optimization of all minimum and transition state electronic structures was performed at this level of theory: Minnesota functional M06, which is a functional that performs well for organometallic systems.[30, 31] Pople's basis set 6-31G(d,p),[32] and Stuttgart-Dresden effective core potential (SDD) for Ni atom.[33, 34] Vibrational frequency calculations were carried out in the same level of theory to confirm convergence–positive eigenvalues for local minima and one single imaginary frequency for the transition states–corrected with the quasi-harmonic approximated frequencies, where frequencies below 100 cm^{-1} were standardized to 100 cm^{-1}.[35] Single-point calculations on the optimized structures with larger basis sets of QZVP for Ni and def2-TZVP for others.[36, 37] SMD implicit solvation with solvent parameters (e.g. 2,2,2-TriFluoroEthanol (TFE)),[38] was done at M06/6-31G(d,p)+SDD level of theory. The reported relative solution free energy, ΔG_{sol}, constitutes the gas-phase single-point and SMD correction, termed as M06/def2-TZVP+QZVP/SMD(2,2,2-TriFluoroEthanol). Thermal and vibrational corrections based on gas-phase were quasi-harmonic approximated vibrations at 80 ºC (353.15 K).[35] The triplet high spin state of Ni(II) for key TSs and intermediates were calculated to be much higher in energy than singlet low spin states with differences in energies ranging from 11.7 to 46.3 kcal/mol (see Supporting Information). The ΔG_{sol} is corrected to consider the passage of 1 atm gas into 1 M in solution, ΔG 1atm→1M as follows:

$$\Delta G^{1atm->1M} = \Delta N \times RTln\,(RT/P)$$

where ΔN is the number of moles of gas change from the reactant to product and RT ln(RT/P) equals to 2.36 kcal/mol at 353.15 K.[39]

Acknowledgements

We acknowledge the Australian Research Council (for Discovery Project DP180101332 to S.G.P. and C.J.T.H.; DECRA

DE210100053 to R.L.), UOW Rita (to C.J.T.H. and R.L.), and UOW VC Fellowship (to R.L.) for research funding. C.B.E.C. acknowledges the UOW IPTA and Matching PhD scholarship. Computational resources were provided by the National Computing Infrastructure (Australia) through the National Computational Merit Allocation Scheme and UOW Partnership Scheme for this work.

Keywords: DFT • cyclization • transmetalation • nickel catalysis • allene •

References and Notes

[1] S. Yu and S. Ma, *Angew. Chem. Int. Ed. Engl.* **2012**, *51*, 3074–3112.
[2] W.-D. Chu, Y. Zhang and J. Wang, *Catal. Sci. Technol.* **2017,** *7*, 4570–4579.
[3] S. Ma, *Acc. Chem. Res.* **2003**, *36*, 701–712.
[4] Y. Liu and M. Bandini, *Chin. J. Chem.* **2019**, *37*, 431–441.
[5] L. Cheng, M.-M. Li, M.-L. Li, L.-J. Xiao, J.-H. Xie and Q.-L. Zhou, *CCS Chem.* **2021**, *3*, 3260–3267.
[6] M. Quan, X. Wang, L. Wu, I. D. Gridnev, G. Yang and W. Zhang, *Nat. Commun.* **2018**, *9*, 2258.
[7] P. K. T. Lo, Y. Chen and M. C. Willis, *ACS Catal.* **2019**, *9*, 10668–10673.
[8] C. Clarke, C. A. Incerti-Pradillos and H. W. Lam, *J. Am. Chem. Soc.* **2016**, *138*, 8068–8071.
[9] H. Panchal, C. Clarke, C. Bell, S. N. Karad, W. Lewis and H. W. Lam, *Chem Commun (Camb)*, **2018**, *54*, 12389–12392.
[10] D.-M. Wang, W. Feng, Y. Wu, T. Liu and P. Wang, *Ange. Chem. Int. Ed.* **2020**, *59*, 20399–20404.
[11] S. M. Gillbard and H. W. Lam, *Eur. J. Chem.* **2022**, *28*, e202104230.
[12] R. Di Sanza, T. L. N. Nguyen, N. Iqbal, S. P. Argent, W. Lewis and H. W. Lam, *Chem. Sci.* **2020**, *11*, 2401-2406.
[13] A. J. Lennox and G. C. Lloyd-Jones, *Angew. Chem. Int. Ed. Engl.* **2013**, *52*, 7362–7370.
[14] C. Zhang, R. Zhao, W. M. Dagnaw, Z. Liu, Y. Lu and Z. X. Wang, *J. Org. Chem*. **2019**, *84*, 13983–13991.
[15] M. Ohashi, H. Saijo, M. Shibata and S. Ogoshi, *Eur. J. Org. Chem.* **2013**, *2013*, 443–447.
[16] C. A. Malapit, J. R. Bour, C. E. Brigham and M. S. Sanford, *Nature*, **2018**, *563*, 100-104.
[17] L. Guo, W. Srimontree, C. Zhu, B. Maity, X. Liu, L. Cavallo and M. Rueping, *Nat. Commun*. **2019**, *10*, 1957.
[18] Interestingly, other substrates that lacked this amide carbonyl also underwent the cyclization reaction.[12]
[19] J. Liu, M. Ling and H. Xie, *Comput. Theor. Chem.* **2020**, *1185*, 112889.
[20] Y. Li, Y. Luo, L. Peng, Y. Li, B. Zhao, W. Wang, H. Pang, Y. Deng, R. Bai, Y. Lan and G. Yin, *Nat. Commun.* **2020**, *11*, 417.
[21] P.-A. Payard, L. A. Perego, I. Ciofini and L. Grimaud, *ACS Catal.* **2018**, *8*, 4812–4823.
[22] P. A. Cox, M. Reid, A. G. Leach, A. D. Campbell, E. J. King and G. C. Lloyd-Jones, *J. Am. Chem. Soc.* **2017**, *139*, 13156–13165.
[23] K. P. Kepp, *Inorg. Chem.* **2016**, *55*, 9461–9470.
[24] X. Zhao, D. Zhang and X. Wang, ACS catal. **2022**, *12,* 1809–1817
[25] Y. F. Yang, X. Hong, J. Q. Yu and K. N. Houk, *Acc. Chem. Res.* **2017**, *50*, 2853–2860.
[26] H.-Y. Sun, S. I. Gorelsky, D. R. Stuart, L.-C. Campeau and K. Fagnou, *J. Org. Chem.* **2010**, *75*, 8180–8189.
[27] C. Legault, *CYLview*, 2009, **1.0b**.
[28] P. Pracht, F. Bohle and S. Grimme, *Phys. Chem. Chem. Phys.* **2020**, *22*, 7169–7192.
[29] M. J. Frisch, G. W. Trucks, H. B. Schlegel, G. E. Scuseria, M. A. Robb, J. R. Cheeseman, G. Scalmani, V. Barone, G. A. Petersson, H. Nakatsuji, X. Li, M. Caricato, A. V. Marenich, J. Bloino, B. G. Janesko, R. Gomperts, B. Mennucci, H. P. Hratchian, J. V. Ortiz, A. F. Izmaylov, J. L. Sonnenberg, Williams, F. Ding, F. Lipparini, F. Egidi, J. Goings, B. Peng, A. Petrone, T. Henderson, D. Ranasinghe, V. G. Zakrzewski, J. Gao, N. Rega, G. Zheng, W. Liang, M. Hada, M. Ehara, K. Toyota, R. Fukuda, J. Hasegawa, M. Ishida, T. Nakajima, Y. Honda, O. Kitao, H. Nakai, T. Vreven, K. Throssell, J. A. Montgomery Jr., J. E. Peralta, F. Ogliaro, M. J. Bearpark, J. J. Heyd, E. N. Brothers, K. N. Kudin, V. N. Staroverov, T. A. Keith, R. Kobayashi, J. Normand, K. Raghavachari, A. P. Rendell, J. C. Burant, S. S. Iyengar, J. Tomasi, M. Cossi, J. M. Millam, M. Klene, C. Adamo, R. Cammi, J. W. Ochterski, R. L. Martin, K. Morokuma, O. Farkas, J. B. Foresman and D. J. Fox, Gaussian 16, Rev. A.03, 2016.
[30] Y. Zhao and D. G. Truhlar, *Theor. Chem. Acc.* **2008**, *120*, 215–241.
[31] D. G. Truhlar, *J. Am. Chem. Soc.* **2008**, *130*, 16824–16827.
[32] R. Ditchfield, W. J. Hehre and J. A. Pople, *J. Chem. Phys.* **1971**, *54*, 724–728.
[33] M. Dolg, U. Wedig, H. Stoll and H. Preuss, *Journal Chem. Phys.* **1987**, *86*, 866–872.
[34] A. Bergner, M. Dolg, W. Küchle, H. Stoll and H. Preuß, *Mol Phys.* **1993**, *80*, 1431–1441.
[35] A. V. Marenich, C. J. Cramer and D. G. Truhlar, *J. Phys. Chem. B.* **2009**, *113*, 6378–6396.
[36] F. Weigend, *Phys. Chem. Chem. Phys.* **2006**, *8*, 1057–1065.
[37] F. Weigend and R. Ahlrichs, *Phys. Chem. Chem. Phys.* **2005**, *7*, 3297–3305.
[38] R. F. Ribeiro, A. V. Marenich, C. J. Cramer and D. G. Truhlar, *J. Phys. Chem. B.* **2011**, *115*, 14556–14562.
[39] J. Ho, A. Klamt and M. L. Coote, *J. Phys. Chem. A*. **2010**, *114*, 13442–13444.

10.1002/asia.202300724

WILEY VCH

RESEARCH ARTICLE

Table of Contents

A detailed DFT mechanistic investigation on redox neutral nickel(II)-catalyzed arylative cyclization reactions of a tethered allene-ketone with arylboronic acids. This work highlights that the transformation consists of three key elementary steps: (i) base-free transmetalation, (ii) cationic terminal allene insertion, and (iii) a diastereo- and enantio-determining cyclization step.

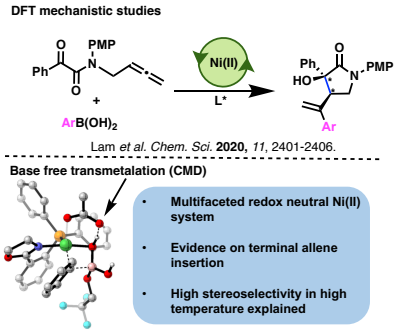

Institute and/or researcher Twitter usernames: @MolHorizons; @HylandChem